



Is ca 24th DAAAM International Symposium on Intelligent Manufacturing and Automation, 2013

## A Novel Implant Regarding Transcondylar Humeral Fractures Stabilization. A Comparative Study of Two Approaches

Mitroi Eduard<sup>a\*</sup>, Vlasceanu Daniel<sup>b</sup>, Bajenescu Titi<sup>b</sup>, Petrescu Horia-Alexandru<sup>b</sup>

<sup>a</sup>*Emergency University Hospital of Bucharest, 050098, Romania*

<sup>b</sup>*University POLITEHNICA of Bucharest, 060042, Romania*

### Abstract

The osteosynthesis of transcondylar humeral fractures is an important branch of the upper limb traumatology. The bone-implant assembly has to be strong enough to resist the high loads arising during the early rehabilitation program, while keeping the soft tissue stripping to a minimum. Using the finite element method, this study compares two alternatives of stabilization of this kind of fractures by means of a new type of implant, less expensive than the existing locking plates and, more importantly, minimally-invasive. This implant comprises two modified cortical screws (one for each column of the distal humerus) and a Kirschner wire (or a partial threaded screw) which locks the screws transversally at the epiphysis. The screws can be placed in the middle of the columns of the distal humerus or with an eccentricity, immediately under the cortical shell of the bone. Using data from distal humerus CT scans, two CAD (Solidworks) models of the bone and implants were produced, imported, edited, loaded and analysed in a finite element analysis program (Ansys). The results indicate that the subcortical placement of the screws is more favorable than the intracancellous one, leading to increased stiffness of the bone-implant assembly. This stage the first refinement of this method and this study will be followed by computer, in-vitro and clinical studies, comparing the behavior of this alternative to the existing standard implants.

© 2014 The Authors. Published by Elsevier Ltd. Open access under [CC BY-NC-ND license](https://creativecommons.org/licenses/by-nc-nd/4.0/).

Selection and peer-review under responsibility of DAAAM International Vienna

Keywords: Humeral transcondylar fractures; osteosynthesis; finite element method; safety factor;

### 1. Introduction

The humeral palette fractures are among the most problematic fractures of the upper limb and their surgical treatment, when required, presents special challenges. Several factors contribute: the uneven local anatomy, the significant cartilage covering of the distal epiphysis, the location of the fracture line, frequently distal, as well as the

\* Corresponding author. Tel +40721525958  
E-mail: [edimitroi@yahoo.com](mailto:edimitroi@yahoo.com)

low bone mineral density of the elderly, who usually suffer this kind of fractures. During the mandatory early rehabilitation high loads are transferred through the fracture zone by the implanted assembly. The gold standard treatment is the osteosynthesis with two parallel or orthogonal locking plates with screws, especially in comminuted fractures. The main disadvantage of this treatment is the extensive surgical approach it necessitates, which becomes obviously excessive in transcondylar fractures. The alternative in this case is the osteosynthesis with two triangulation screws, but this method provides far less stiffness than the standard method. To address this shortcoming, we have developed a new osteosynthesis device for transcondylar distal humerus fractures, consisting in two modified cortical bone screws and a 3mm Kirschner wire (or a 3mm partially threaded screw). This locks the aforementioned screws transversally, thus increasing the contact area between the osteosynthesis device and the fragile distal epiphyseal bone, which is susceptible to refracturing during the rehabilitation program.

The aim of this study is to compare the efficiency of two configurations of this new osteosynthesis by means of the finite element method, in terms of relative strength and stiffness of the assembly and impact on the surrounding bone tissue.

## 2. The method

### 2.1 The implant and the two placement alternatives

The two modified screws have almost identical geometry, differing only in their length. Each screw has a threaded proximal end, a cylindrical body with a diameter equal to that of the thread and a larger cylindrical distal end required for the locking and guiding tools. This end also has an oblong hole that accommodates the locking screw or wire and a threaded hole designed for an optional mini-blocking screw and also for the guiding devices (figures 1, 2).



Fig. 1. The 3D view of a threaded pin with its locking mini-screw.

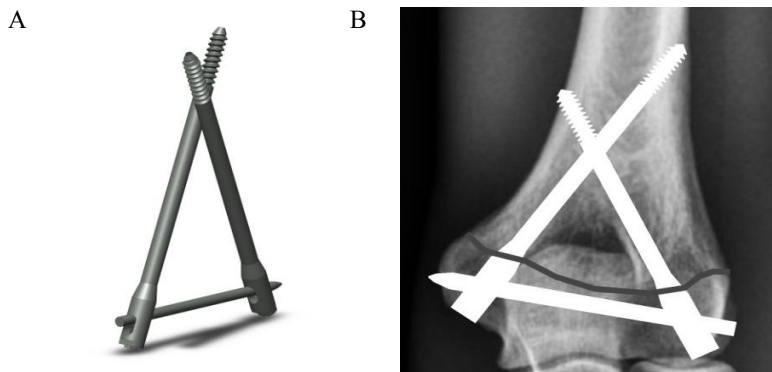


Fig. 2. Two modified screws with a locking Kirschner wire (A). Anteroposterior Rx-ray of the in-situ implants (B).

We considered two ways of positioning these screws in the distal humerus, each of them presenting advantages and drawbacks. The first alternative (A) involves the central positioning of the screws in the two columns of the distal humerus, the screws being enclosed by cancellous bone. The advantage here is the solid distal anchorage, each screw being surrounded by at least 4-5 mm of bone tissue (figure 4A). The contact area between the implant and the problematic distal epiphyseal bone is greatest in this configuration. When the bone is very weak, however, the screws anchored in the metaphyseal cancellous bone could generate microfractures with subsequent assembly deterioration.

In the second alternative, the screws run through the metaphysis subcortically, immediately below the shell of compact bone. On the lateral side of the humerus, they rest on compact bone laterally, anteriorly and posteriorly. This positioning cannot always be achieved on the medial side, where the medial epicondyle is broader in the sagittal plane than both its lateral counterpart and the lateral crest. However, the surgeon could insert the medial screw either anteriorly or posteriorly in order to ensure some degree of compact bone-implant contact. This configuration is less susceptible to metaphyseal refractures but brings about the potential deterioration of the distal fragment, given the decreased contact between the screws and the distal fragment (figure 3).

The study compares these two alternatives by means of a computer simulation using the finite element method. One bone-implant model was built for each variant, edited and loaded with the joint reaction forces typically encountered during elbow postoperative rehabilitation. The results of the analysis were interpreted according to several criteria in order to assess which implant alternative has the more favorable behavior.

## 2.2 The 3D modeling of the humerus and implants

The 3D model of the distal humerus was developed in Solidworks using the CT scan images of a right humerus. The model consists of two bonded parts: the compact bone (the outer part) and the cancellous bone (the inner part), the latter being present only in the epiphyseal and metaphyseal regions of the distal humerus. The reasons for this detail are the important differences in mechanical properties of the two kinds of bone [4]. We considered a transcondylar fracture (or low supracondylar), with an uneven course and an interfragmentary gap of 0.5mm. We used an unstable fracture in order to better assess the performance of implants (especially differential performance) [3,4, 6, 8, 9], even though they intended usage is for stable fractures only.

After positioning the implants (the screws and the Kirschner wire) in the distal humerus according to the two aforementioned configurations (A and B), the cavities needed for the bone-implant matching were created in the bone models.

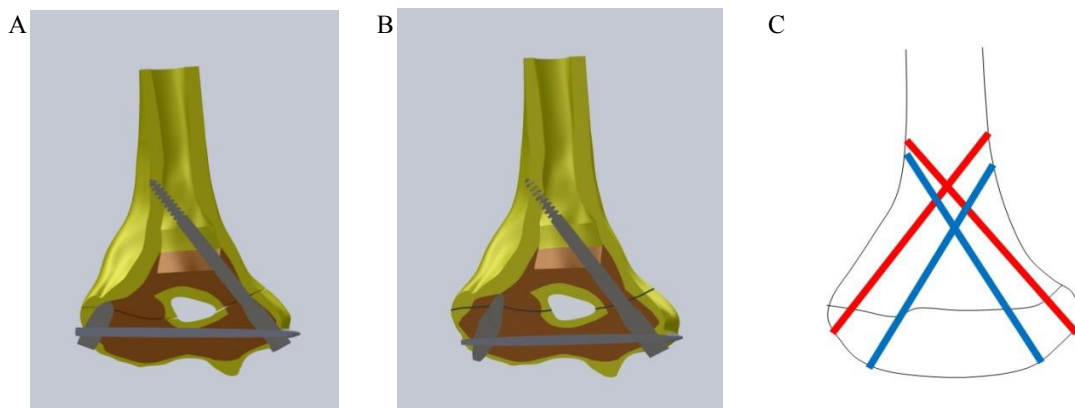


Fig. 3. A, B - Coronal sections through the humerus and implants in Solidworks: model A (A); model B (B); C - sketch showing the position of the screws in both models (superimposed for easier comparison).

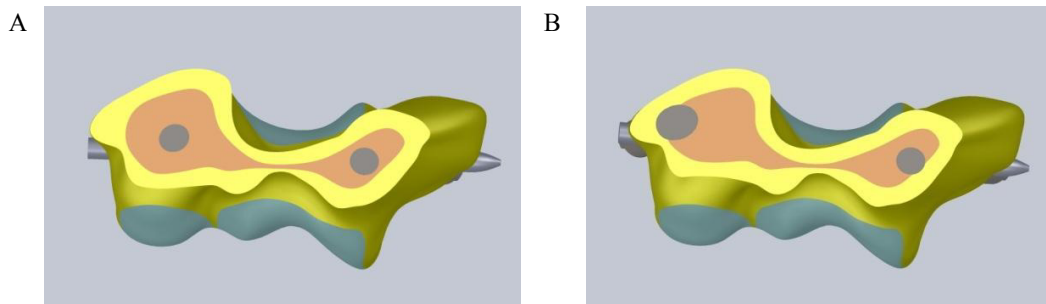


Fig 4. Transversal sections through the model A (A) and model B (B) showing the placement of the screws.

Next the models were imported into Ansys 14.0, a state of the art finite element analysis program. The finite element type used for discretization of the model (SOLID187) has ten nodes and three degrees of freedom for each node. The discretization used a small element size and slow size transitions in order to provide better accuracy of the results [4,10]. Local mesh parameters were adjusted to ensure a realistic behaviour and reduce the occurrence of artifacts, given the irregularities of the humerus and of the contact areas between implants and bone.

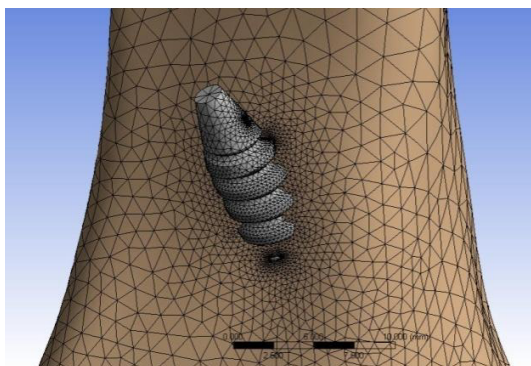


Fig. 5. The mesh refinement for the exit area of a screw (thread).

### 2.3 The test set-up

The materials used for the implants and humerus have the mechanical properties of titanium alloy, cortical bone and cancellous bone. These data are exposed in the table 1. Given the large range of the bone mechanical properties as a function of density, we have chosen those corresponding to a moderately demineralized bone [3,7].

Table 1. The mechanical properties of the materials used in the analysis.

	Young's modulus (MPa)	Poisson's ratio	Tensile yield stress (MPa)	Compressive yield stress (MPa)	Tensile ultimate strength (MPa)	Compressive ultimate strength (MPa)
Titanium alloy	96000	0.36	930	930	1070	1070
Compact bone	13000	0.3	100	120	110	140
Cancellous bone	600	0.2	5	5	6	6

For each alternative the model consisted of seven bodies - three implants (the screws and the Kirschner wire), the proximal humeral fragment and the distal fragment (each composed of a shell of compact bone and an inner cancellous part) - and the contact surfaces between them. Each screw meets the four osseous bodies and the locking Kirschner wire. The compact and cancellous bodies are bonded (no sliding or separation between faces or edges is allowed) for each fracture fragment (proximal and distal). The locking wire meets and is linked to the two parts of the distal fragment. In order to make for an easier assessment of implant performance, no contact was modeled between the proximal and distal bone fragments, a situation intended to simulate an unstable fracture. The connections between implants and bone were also modeled with “bonded” feature.

The subsequent phase was the proper set-up of the implant-bone system for each of the two options. The proximal humeral fragment was fixed at its cranial end, about 10 cm from joint line. Generally, the most important forces operating on the elbow joint are located in the sagittal plane, while those located in the coronal and axial planes are often negligible [1]. The value and orientation of the forces are distinct for the trochlear and capitellar surfaces and these parameters are a function of elbow position and the instant of movement (the greatest values being obtained at the ultimate flexion and extension) [1,2,5]. Eight load cases have been considered for each model. The table No. 2 illustrates the reaction forces and their orientation in the sagittal plane during elbow movements for 10N load at the wrist region [1]. This value (10N) corresponds to the typical order of magnitude of the forces developed during the elbow postoperative rehabilitation.

Table 2. The magnitude and orientation of the reaction forces in the sagittal plane; the second values are the angle between the direction of the force and humeral caudocranial axis; a negative angle indicates an anterior direction.

Grades	Flexion		Extension	
	Trochlea	Capitulum	Trochlea	Capitulum
0°	114/-20°	-8/-8°	122/-13°	86/0°
30°	102/4°	135/19°	122/-13°	86/28°
90°	55/30°	80/75°	172/5°	86/83°
120°	55/30°	66/105°	206/33°	86/111°

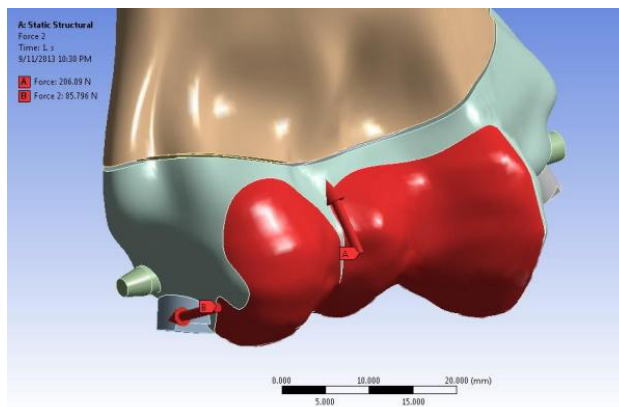


Fig. 6. The orientation of the forces acting on capitulum and trochlea at 120° during extension.

### 3. Results and discussion

The detection and documentation of susceptibility for fracture displacement, implant failure and/or bone fragments refracturing (and consecutive cutting out of the implants) are endpoints often pursued in clinical and laboratory studies [6, 8, 9]. In order to asses susceptibility for these types of failure, we monitored the following

output, for both models: the displacement between the two bone fragments, von Mises equivalent stresses, normal and shear stresses, (for all eight load cases (at  $0^\circ$ ,  $30^\circ$ ,  $90^\circ$  and  $120^\circ$ , during flexion and extension). The stress maps use absolute values (MPa) for the titanium alloy and relative values for the bone (the safety factor (sf), indicating the ratio between the tensile yield stress,  $S_{yield}$ , and the maximum principal stress,  $\sigma_1$ ).

The most significant results are displayed in figures 7 and 8.

The relative displacements between the proximal and distal bone fragments were insignificant and almost identical in the two models. The maximum anteroposterior and craniocaudal translation and the deflection of the distal fragment with corresponding interfragmentary gap closing were 0.08mm and  $0.5^\circ$  respectively, too small to preclude the fracture healing in vivo.

The maximum equivalent stress was recorded on the lateral screw for both models, near the fracture gap, during flexion at  $0^\circ$ : 186.8 MPa for model A and 167.4 MPa for model B. Both values are far below the titanium alloy yield strength (930 MPa), which makes fatigue failures also improbable. In the majority of load cases the values for maximum equivalent stress in the implants were higher in model A (figure 7). The difference was significant in at least two cases: flexion and extension from  $120^\circ$  (e.g. in extension from  $120^\circ$  the difference was 83%).

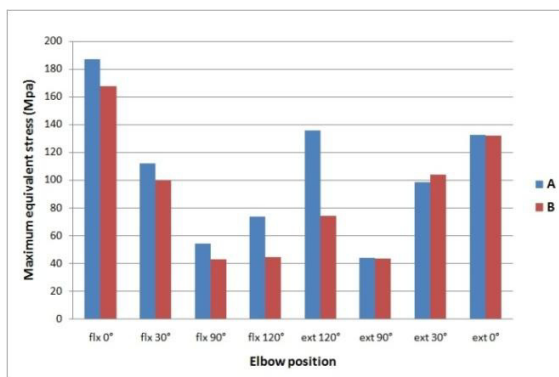


Fig. 7. Comparative maximum equivalent stress in the implants in the two models.

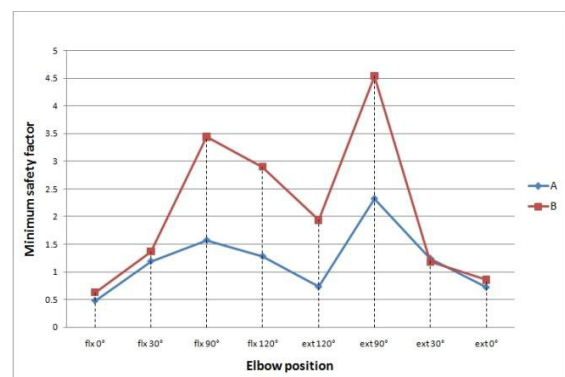


Fig. 8 Minimal values for safety factor (both models).

The normal stress values in the bone fragments were lower (i.e. safety factors were higher) in all load cases for model B except the extension from  $30^\circ$  (figure 8). These differences, favoring model B were significant in at least four cases: flexion and extension from  $90^\circ$  and  $120^\circ$  (figure 8). The safety factor was less than unity in several cases: flexion and extension from  $0^\circ$  and extension from  $120^\circ$  (at the extremes of the range of motion). The overstressed areas are located (in both models and in all load cases) in the cancellous bone of the proximal fragment, adjacent to the fracture gap, at the bone-screw interface. The strength of the cancellous bone in these areas is critical for the overall performance of the implant; the overstressing here under typical loads is precisely the reason why this kind of implant is not recommended for use in unstable fractures. The differences between the sf values for the two models were expected: in model A the screws are anchored in cancellous bone, whereas in model B they are anchored in stronger cortical bone.

In the opening chapter we mentioned the potential disadvantage of the subcortical positioning of the screws: the fracturing of the distal fragment, because of its worse stabilization (with consequent greater stress). The maximum stress values in the distal fragment are indeed greater in model B in all loading situations, but since these stress areas are located in the cortical bone, the resulting relative stress values are lower (higher sf values), which renders the refracture of the distal fragment less likely. The safety factor maps describe the two patterns more clearly (figure 9).

In summary, alternative B, involving the subcortical positioning of the screws, appears to be the better option. The maximum stress values for both the implant and bone are higher in model A. The distal fragment secondary fracture, the potential disadvantage of the second configuration (B), is unlikely. For both models, the sites prone to refracture are the metaphyseal areas surrounding the screws. This is especially likely during extreme flexion

and extension, which reinforces the common wisdom that in these circumstances special attention has to be paid during the rehabilitation program.

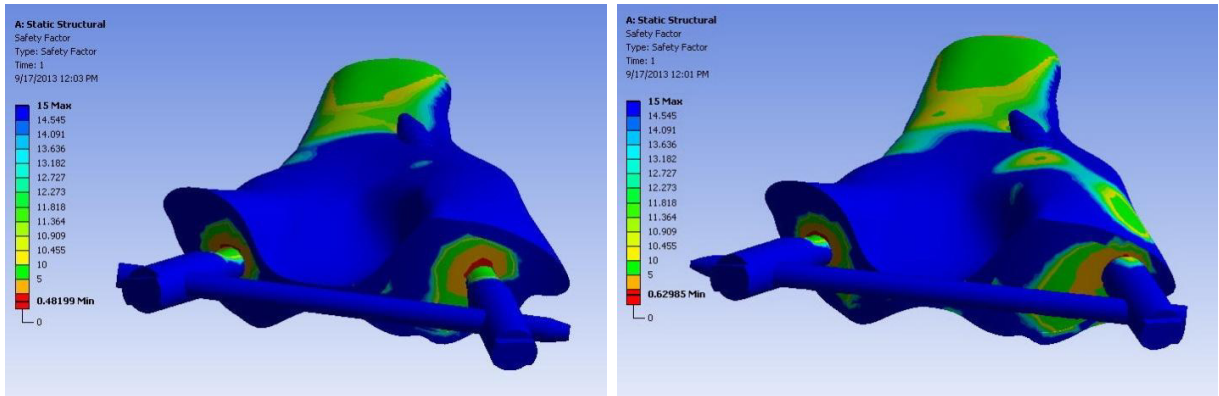


Fig. 9. Contour bands for safety factor in flexion from 0° after removing the distal fragment, in order to illustrate the stress in the cancellous and compact bone of the proximal fragment: model A (left); model B (right).

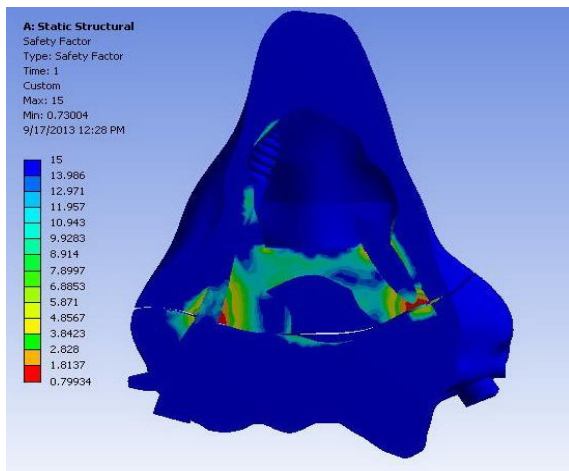


Fig. 10. Coronal section through the humerus-implants assembly in model A, illustrating the critical areas around the screws (safety criterion during extension from 120°).

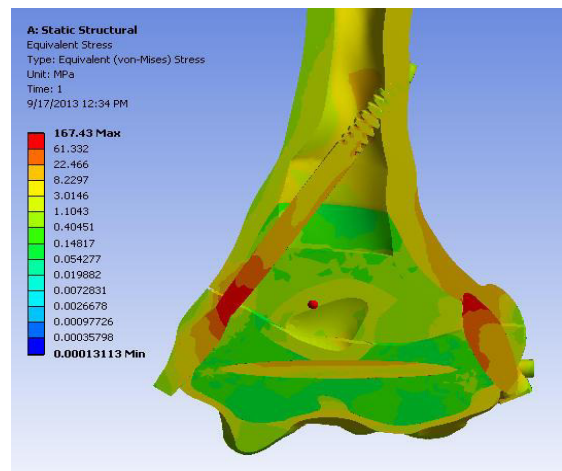


Fig. 11. Coronal section through the humerus-implants assembly in model B, showing the most stressed areas on the screws (the equivalent stress in flexion from 0°).

Not unlike laboratory tests, this study has several limitations. The model of the bone did not take into account the gradual transition from compact to cancellous tissue. Moreover, the cancellous bone is not isotropic, nor does it possess a homogenous structure, being denser in the high load areas. The materials used in the analysis for bone tissue were homogenous and isotropic, due to the sparse preexisting data and the additional technical difficulties such details would have added to the analysis. The most important limitation regarding the bone modeling is the varying thickness and strength of demineralized compact bone, parameters which greatly influence the stiffness of the bone-implant assembly.

#### 4. Conclusion

This study presents a novel osteosynthesis device for transcondylar humeral fractures as an alternative for the more expensive and invasive locking plates and compares the performance of two of its implantation alternatives using the finite element method. The results of this finite element analysis reinforce the somewhat expected premise that the subcortical placing of the screws provides greater stiffness under the high loads imposed by elbow movements. The study also confirms the dangers brought about by the extremes of the range of motion. These results are to be confirmed by the forthcoming laboratory tests and future clinical studies.

#### References

- [1] Amis AA, Dowson D, Wright V. Elbow joint force predictions for some strenuous isometric actions. *J Biomech* 1980;13:765–75.
- [2] Askew L.J., An K.N., Morrey B.F., Chao E.Y.: Isometric elbow strength in normal individuals. *Clin. Orthop* 1987; 222:261.
- [3] Diederichs G., Issever A.S., Greiner S., Linke B., Korner J., Three-dimensional distribution of trabecular bone density and cortical thickness in the distal humerus, *J Shoulder Elbow Surg* (2009) 18, 399-407.
- [4] Lin CL., Lin YH, Chen ACY, Buttressing angle of the double-plating fixation of a distal radius fracture: a finite element study, *Medical and Biological Engineering and Computing* 44 (2006), 665-673.
- [5] Nobuta S.: Pressure distribution on the elbow joint and its change according to positions, *J. Jpn. Soc. Clin. Biomech. Res.* 1991; 13:17
- [6] Penzkofer R., Hungerer S., Wipf F., Oldenburg G., Augat P, Anatomical plate configuration affects mechanical performance in distal humerus fractures, *Clinical Biomechanics* 25 (2010) 972–978.
- [7] Sanyal A, Gupta A, Bayraktar H, Kwon RY, Keaveny T, Shear strength behaviour of human trabecular bone, *Journal of Biomechanics* 45 (2012) 2513–2519.
- [8] Shimamura Y, Nishida K, Imatani J, Noda T, Hashizume H, Ohtsuka A, Ozaki T, Biomechanical Evaluation of the Fixation Methods for Transcondylar Fracture of the Humerus: ONI Plate Versus Conventional Plates and Screws, *Acta Med. Okayama*, 2010 Vol. 64, No. 2, pp. 115-120.
- [9] Stoffel K , Cunneen S, Morgan R, Nicholls R, Stachowiak G, Comparative Stability of Perpendicular Versus Parallel Double-Locking Plating Systems in Osteoporotic Comminuted Distal Humerus Fractures, *Wiley InterScience Inc. J Orthop Res* 26:778–784, 2008.
- [10] Taheri NS, Blicblau AS, Singh M, Comparative study of two materials for dynamic hip screw during fall and gait loading, *Journal of Orthopaedic Science* 16 (2011); 805-813.